

DOI: 10.1002/celec.201402127

Special
Issue

Investigation of Electron Transfer by *Geobacter sulfurreducens* Biofilms by using an Electrochemical Quartz Crystal Microbalance

Jerome T. Babauta,^[a] Christopher A. Beasley,^[b] and Haluk Beyenal^{*[a]}

Both the short- and long-term electron-transfer processes of electrode-respiring *Geobacter sulfurreducens* biofilms are demonstrated by using an electrochemical quartz crystal microbalance (QCM). The QCM monitors the frequency shift from the initial resonant frequency (background) in real time, while the current increases, because of biofilm growth. In the short term, the frequency shift is linear with respect to current for the biofilm. In long-term biofilm growth up to the exponential phase,

a second linear region of frequency shift with respect to current is observed. In addition to the frequency shift response at constant polarization, the frequency shift response is coupled to cyclic voltammetry experiments. During cyclic voltammetry, a reproducible, negative increase in frequency shift is observed at oxidizing potentials. The results suggest that a QCM can be used in applications in which it is useful to find the most efficient current producer.

1. Introduction


Electrode-respiring *Geobacter sulfurreducens* biofilms are widely used as a model electrochemical system to gain a mechanistic understanding of how electrons are conducted to the extracellular space within a biofilm.^[1] Multiple studies have elucidated the importance of relating the self-secreted electron-transfer mediators of *G. sulfurreducens* biofilms, which are responsible for extracellular electron transfer, to electrochemical techniques, such as cyclic voltammetry (CV).^[2] Such studies relate the metabolic state of the biofilm to CV through either nutrient removal/addition or gene manipulation. Additionally, we previously reviewed the use of coupled electrochemical techniques as promising methods to study electrochemically active bacteria.^[3] For example, monitoring biofilm formation through microscopy has yielded valuable information on the state of biofilm self-secreted electron-transfer mediators and local physicochemical environments.^[4] Another useful coupled technique to study bacterial attachment and biofilm formation is the quartz crystal microbalance (QCM) technique,^[5] which has


been used previously to study the attachment of anodic bacteria to anodes for microbial fuel cells^[6] or, more generally, bioelectrochemical systems.^[7] QCM has also been used to study protein–protein interactions of redox enzymes of *Shewanella oneidensis* involved in extracellular electron transfer.^[8] What has been common to these QCM studies is the decreasing frequency shift of the oscillating quartz crystal with increasing bacterial attachment, which is expected for increased mass loading (see the Experimental Section).^[9] However, there is difficulty in relating the frequency shift to attached mass through the Sauerbrey relationship,^[10] because of the viscoelastic nature of biofilms.^[11] Although complicated by viscoelastic properties, QCM studies would yield critical insights into the coupling of electron-transfer and mass-transfer gradients operating in *G. sulfurreducens* biofilms.^[12]


G. sulfurreducens biofilms have been considered and treated as conductive, metallic-like films adhering to an electrode surface.^[13] However, it is also important to consider the commonly accepted archetype in which biofilms are thought of as cells surrounded by extracellular polymeric substances or simply biopolymers.^[11] Therefore, we looked to common examples of conductive polymeric films and found similarity in electrodeposited polyaniline (PANI) films for their ability to behave with metallic-like conductivity.^[14] Although chemically distinct from *G. sulfurreducens* biofilms, electrodeposited PANI films suffer from similar electron-transfer limitations, such as mass-transfer gradients within the film, and advantageously have a well-established QCM-based literature. Of particular importance is the observation of the ingress/egress of charged species, net neutral species, and solvent that Hillman et al. theoretically demonstrated in polymer films through the coupling of CV and QCM.^[15] Considering that *G. sulfurreducens* biofilms are either redox-gradient driven or metallic-like, while suffering mass-transfer limitations, we believe it is important to address

[a] J. T. Babauta, H. Beyenal
The Gene and Linda Voiland School of Chemical Engineering and
Bioengineering, PO Box 646515, Washington State University
Pullman, WA 99164-6515 (USA)
E-mail: beyenal@wsu.edu

[b] C. A. Beasley
Gamry Instruments, Inc.
734 Louis Dr, Warminster, PA 18974 (USA)

 Supporting Information for this article is available on the WWW under
<http://dx.doi.org/10.1002/celec.201402127>.

 © 2014 The Authors. Published by Wiley-VCH Verlag GmbH & Co. KGaA.
This is an open access article under the terms of the Creative Commons
Attribution Non-Commercial NoDerivs License, which permits use and
distribution in any medium, provided the original work is properly cited,
the use is non-commercial and no modifications or adaptations are
made.

 An invited contribution to a Special Issue on Biofuel Cells

whether these biofilms behave similar to conductive polymer films in the coupling of CV and QCM. The goals of this research were 1) to investigate the electron-transfer processes of *G. sulfurreducens* in biofilms growing on a QCM surface and relate the biofilm growth to the frequency shift, and 2) to compare the biofilm results with well-known control systems as a reference.

Herein, we quantified the frequency shift during both the initial growth and exponential growth of electrode-respiring *G. sulfurreducens* biofilms. Biofilms were grown on a QCM electrode under constant polarization. The QCM monitored the frequency shift from the initial resonant frequency (background) in real time, while the current increased from biofilm growth. In addition to the frequency shift at constant polarization, we coupled the frequency shift to CV and demonstrated the similarity of the biofilm to electrodeposited PANI films and its dissimilarity to copper deposition. We also considered the viscoelastic nature of the biofilm compared with those of both copper and PANI films by using the deviation between the series resonant frequency shift and the parallel resonant frequency shift. Finally, we used ferricyanide reduction, a non-film-forming electrochemical reaction, as a control.

2. Results and Discussion

2.1. Biofilm Growth on QCM Electrodes

Similar to previous bioelectrochemical systems, once the inoculum was added to the QCM cell, the cells attached to the electrode face that was exposed to solution and the current began to increase. Figure 1 shows the typical current response of electrode-respiring *G. sulfurreducens* biofilm growth, consisting of a lag phase, an exponential phase, and a stationary phase, over a 115 h period (≈ 5 days).^[16] The steady-state current for the QCM electrode reached an average value of $(127 \pm 8) \mu\text{A}$ ($n=3$) when polarized to $0 \text{ mV}_{\text{Ag}/\text{AgCl}}$. The current re-

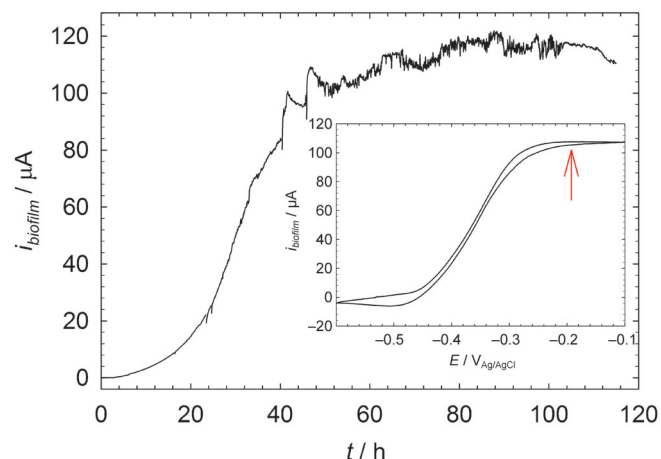


Figure 1. Typical electrode-respiring *G. sulfurreducens* biofilm growth on the QCM electrodes. The inset shows a cyclic voltammogram after 115 h of growth. The red arrow indicates the limiting current. Both the current response and the cyclic voltammogram are characteristic of *G. sulfurreducens* biofilms respiring on electrodes polarized at the limiting current (i.e. above $\approx -200 \text{ mV}_{\text{Ag}/\text{AgCl}}$).

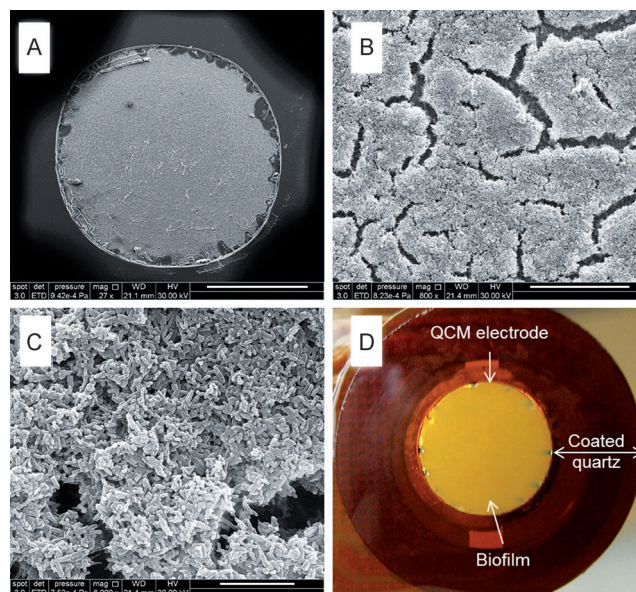


Figure 2. SEM images of a *G. sulfurreducens* biofilm grown on a QCM electrode at A) $27\times$ (scale bar: 3 mm), B) $800\times$ (scale bar: $100 \mu\text{m}$), and C) $6000\times$ (scale bar: $10 \mu\text{m}$) magnification. D) Photograph of the biofilm before SEM sample preparation. *G. sulfurreducens* biofilms on QCM electrodes appeared to cover the electrode surface uniformly.

sponse and cyclic voltammogram (inset in Figure 1) obtained by using QCM electrodes were characteristic of *G. sulfurreducens* respiring on electrodes polarized at the limiting current (i.e. above $\approx -200 \text{ mV}_{\text{Ag}/\text{AgCl}}$). During biofilm growth, the QCM electrodes were simultaneously operated while capturing current response or cyclic voltammograms. This simultaneous operation allowed us to obtain resonant frequency information and the electrochemical activity of the biofilm at the same time.

As shown in Figure 2, the biofilm only grew on the QCM electrode; this demonstrated that the only electron acceptor was the electrode. Figure 2A shows that the biofilm generally grew uniformly across the QCM electrode surface. Details of the biofilm surface are shown at magnifications of $800\times$ and $6000\times$ in Figure 2B and C, respectively. Owing to the scanning electron microscopy (SEM) sample preparation, cracks appeared and revealed the dense packing of cells in the biofilm; these are expected.^[12a] Figure 2D shows the QCM insert, which consisted of an AT-cut quartz disk, a 7 mm gold-coated quartz surface (the QCM electrode), and resin-coated quartz (inert). The pink hue on the QCM electrode is typical of an attached *G. sulfurreducens* biofilm. The SEM and digital camera images shown in Figure 2 demonstrate the successful growth *G. sulfurreducens* biofilms on QCM electrodes, which allow us to study the QCM response due to the growth of electrode-respiring *G. sulfurreducens* biofilms.

2.2. Initial Biofilm Growth

Upon the addition of cells to the QCM cell, there was an immediate response in both the current and series resonant fre-

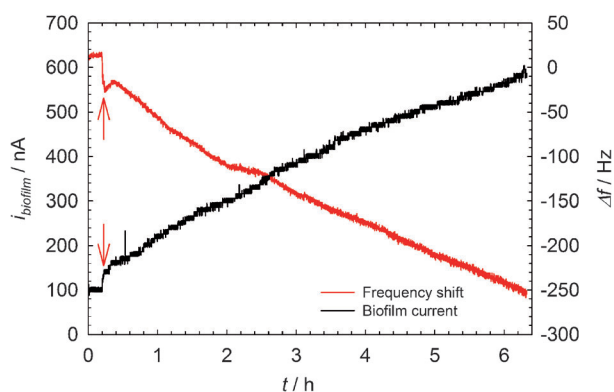


Figure 3. The current response and frequency shift during the initial biofilm growth on the QCM electrode. The red arrows indicate the time of inoculation. Upon inoculation, both current and frequency shift responded sharply.

quency of the oscillating crystal, which indicated cell attachment and electron transfer. Figure 3 shows the current response and frequency shift upon the addition of cells. Initially, the current increased sharply from 100 to 130 nA with the addition of cells to the QCM cell. Simultaneously, the frequency shift dropped sharply by 30 Hz from a baseline frequency shift of 15 Hz. Within 6 h, the current and frequency shift reached values of 580 nA and -250 Hz, respectively. We expected that the frequency shift would decrease as the current increased. As cells attached and the biofilm grew, the mass loading on the oscillating crystal increased and caused the resonant frequency to decrease. As more biofilm attached, the frequency shift decreased further, which indicated that, even for small current responses ($< 1 \mu\text{A}$), the QCM response could be detected. However, it was not immediately clear from the results shown in Figure 3 what relationship current and frequency shift held for what was essentially electrodeposition of *G. sulfurreducens* biofilms. Bressel et al. observed through simultaneous QCM and CSLM measurements that essentially a monolayer of biofilm ($< 5 \mu\text{m}$ thickness) derived from a drinking water source yielded a frequency shift of -780 Hz.^[5b] Rest potential measurements showed that the QCM response occurred only after irreversible attachment of cells to the surface and not during reversible attachment. Similar behavior was observed in mixed-culture wastewater biofilms.^[7] Therefore, we believe that, in our case, the immediate change in frequency shift and current correspond to irreversible attachment of *G. sulfurreducens* cells to the QCM electrode. As *G. sulfurreducens* relies on direct electron transfer to solid surfaces,^[16,17] it is reasonable to conclude that cells immediately and irreversibly attach to the QCM electrode surface to continue respiration and survive.

We looked to similar electrochemical analogues and found that electrodeposition of conductive polymeric films could provide both similar and contrasting insights into the QCM response observed in Figure 3. Electrodeposition of thin conductive polymeric films, such as PANI, is generally studied by using monomers that are activated anodically and form complex polymer chains on the electrode surface.^[18] Figure 4 shows the electrodeposition of PANI from a solution of aniline HCl under

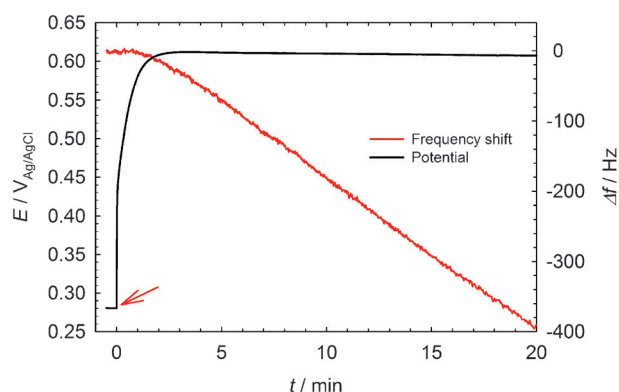


Figure 4. Electrode potential and frequency shift during the electrodeposition of PANI under galvanostatic control at $1 \mu\text{A}$ for 20 min. The total charge passed was 1.2 mC, including the initial charging current. The red arrow indicates when the $1 \mu\text{A}$ current was applied.

galvanostatic control. The onset of PANI electrodeposition was slightly below $0.6 \text{ V}_{\text{Ag}/\text{AgCl}}$ after 1 min of constant current. The rise in potential from $0.28 \text{ V}_{\text{Ag}/\text{AgCl}}$ to slightly below $0.6 \text{ V}_{\text{Ag}/\text{AgCl}}$ reflects the charging of the electrode surface and is indicative of transient, background, non-faradaic processes. During this initial transient phase, the initial resonant frequency of the oscillating crystal did not change; subsequently, the frequency shift remained stable at about 0 Hz. The change in electrode potential without a frequency shift response affirms that series resonant frequency changes occur only when additional mass binds to the surface. Once the electrode potential stabilized (beyond the initial transient phase), the anodic activation of the aniline monomer and subsequent electrodeposition began. After 20 min, the frequency shift decreased from baseline to -390 Hz, which was qualitatively similar to previous electrodeposited PANI on gold QCM electrodes.^[19] When we compare PANI film growth and the biofilm growth in Figures 3 and 4, we can simply state that film growth was accompanied by a decrease in frequency shift and, in this sense, the two were similar. However, because biofilms are preferably grown potentiostatically and PANI galvanostatically (although deposition using CV is common), this implies a fundamental difference in film propagation between the two. The electrodeposition of PANI was controlled and limited by current. Higher current gives faster film propagation. The linear frequency shift response with time in Figure 4 indicated that the total charge passed and the frequency shift were proportional. Thus, the amount of mass deposited depended entirely on the total charge transferred. In contrast, initial *G. sulfurreducens* biofilm growth was not limited by current; instead, it was limited by other, unspecified, metabolic processes, such as the development of self-secreted electron-transfer mediators/structures.^[12a,17] Thus, if *G. sulfurreducens* biofilms were grown galvanostatically, the set current would have to be incrementally and continuously adjusted to the new current, while monitoring the electrode potential. It follows then that the potentiostatic mode is more practical. For current to increase, the number of sites facilitating electron transfer must have increased with increasing cell density and expression of biopoly-

mers during initial growth. The initial contact of single cells of *G. sulfurreducens* DL-1 with an electrode surface was estimated to generate a current of 92 fA.^[20] As current is a necessary prerequisite for *G. sulfurreducens* biofilms on electrodes, propagation of the biofilm must be fundamentally a flux-based mechanism of continuous respiration and electron transfer to the electrode.

Figure 5 A,B shows the differences between the biofilm and PANI QCM responses: current is integrated over time and normalized to total moles of electrons transferred (N_{e^-}). For similar amounts of N_{e^-} , the frequency shift of the biofilm was approximately fivefold smaller than the PANI frequency shift. The bio-

film frequency shift shown in Figure 5 A was nonlinear with respect to N_{e^-} and affirmed that the total charge passed was not controlling. The PANI frequency shift shown in Figure 5 B was linear (slope, $-16.6 \text{ Hz nmol}^{-1}$; $R^2=0.99$) with respect to N_{e^-} . Thus, PANI propagation required stoichiometric amounts of electrons to be deposited. When we consider that the biofilm (and individual cells within it) requires a certain amount of electron flux,^[21] we expect frequency shift to be linear with current. Figure 5 C confirms our expectation: the frequency shift of the biofilm deposition process was linear with respect to current (slope, -0.52 Hz nA^{-1} ; $R^2=0.99$). The linear response in Figure 5 C suggests that for *G. sulfurreducens* biofilms the magnitude of the slope could be used to assess the ability of attached cells to transfer electrons to an electrode surface. If we consider that an individual cell will generate an individual current of about 100 fA, the slope of -0.52 Hz nA^{-1} can be converted into a per cell basis of $-5.2 \times 10^{-5} \text{ Hz/cell}$. A slope of this magnitude is unreasonably small for a cell, considering that the theoretical calibration factor for the quartz crystals here is $226 \text{ Hz cm}^2 \mu\text{g}^{-1}$ (assuming a Sauerbrey relationship). The frequency shift magnitudes for initial biofilm growth are more closely related to the adsorption of lipid bilayers,^[8] which suggests that the slope is tracking the adhesion of biopolymers to the QCM electrode surface.

2.3. Exponential Biofilm Growth on the QCM

Young *G. sulfurreducens* biofilms are markedly different from older, thicker biofilms, because of the increasing density of a biofilm with time.^[12b] We would expect the accumulation of extracellular polymeric substances to change the physical structure of the biofilm and result in a change in frequency shift. When the biofilm grew beyond the current of 600 nA, or only 0.5% of maximum current, we observed a change in the frequency shift/current slope. The extended frequency shift is shown in Figure 6. Beginning at approximately $2 \mu\text{A}$, the initial slope deviates and shifts to a new linear region. Figure 6 shows two biological replicated biofilms: biofilm-1 and biofilm-2. The slopes for biofilm-1 and biofilm-2 were -33 and

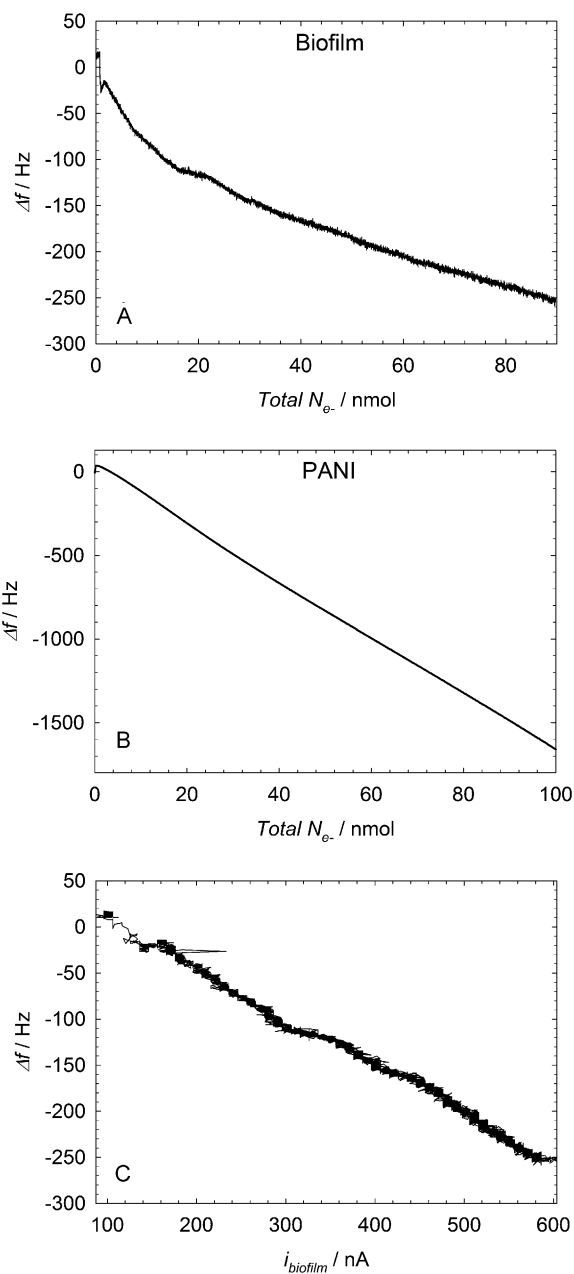


Figure 5. Frequency shift in response to the total moles of electrons passed (N_{e^-}) for A) the initial growth of *Geobacter* biofilm and B) PANI. C) Frequency shift in response to current for initial biofilm growth showing a linear trend (slope, -0.52 Hz nA^{-1} ; $R^2=0.99$).

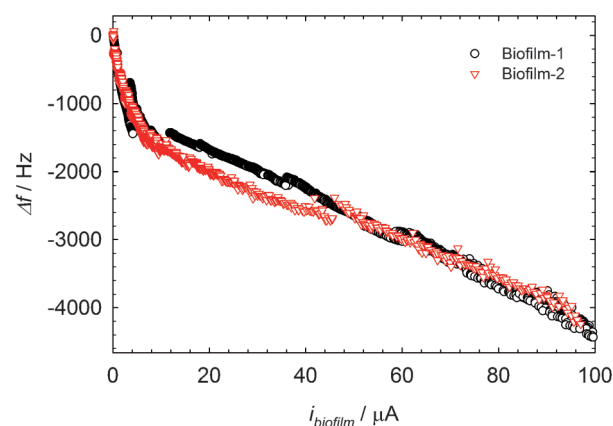


Figure 6. Extended frequency shift/current trend for two *G. sulfurreducens* biofilms up to $100 \mu\text{A}^{-1}$. The slopes for biofilm-1 and biofilm-2 were -33 and $-26 \text{ Hz } \mu\text{A}^{-1}$, respectively.

$-26 \text{ Hz } \mu\text{A}^{-1}$, respectively. The second linear region of the frequency shift/current relationship for the biofilm coincides with the exponential current increase. Compared with the initial trajectory during initial attachment, the slope in the exponential phase decreases over 15-fold, which suggests that more current is produced with less biomass. This point has been stressed previously in the literature: cells are said to “adapt” to respiration on electrodes.^[22] Thus, we can hypothesize that the two linear regimes signify two primary events that occur as biofilms grow and respire on electrodes. First, initial attachment of cells occurs, followed by the conditioning and rapid growth of those cells on the electrode surface. We caution, however, that the interpretation that more current is produced from less biomass may be skewed by cells far from the QCM electrode surface not being detected equally to those directly adjacent to the QCM electrode surface. As Bressel et al. found,^[5b] the addition of further biomass, as indicated by a frequency shift of the QCM, does not result in an equivalent change in rest potential. Although *G. sulfurreducens* biofilms are conductive such that cells are able to respire multiple cell lengths away from the electrode surface,^[23] the mass of those cells may not be observed completely by the QCM. Therefore, it is possible that the switch from the initial slope to the secondary slope represents the transition from a thin (few cell layers) to a thick (multiple cell layers) biofilm. By considering this scenario, both slopes can be used to identify the growth of *G. sulfurreducens* biofilms on QCM electrodes, depending on whether young or older biofilms are used.

2.4. CV

As necessary, during biofilm growth in the QCM cell, polarization could be stopped and we could run CV. Interestingly, we observed a resonant frequency response as the biofilm was oxidized and reduced. In Figure 7A, three cyclic voltammograms are shown, corresponding to before inoculation (no biofilm), 11 h after inoculation, and 22 h after inoculation. The current/potential response was typical of early stages of *G. sulfurreducens* biofilm growth.^[2c] When there was no biofilm, the fre-

quency shift/potential response was flat and unchanging. After 11 h, a slight decrease in oxidizing potentials to -19 Hz was observed. After 22 h, the frequency shift decreased further to -100 Hz . This response was characteristic of all *G. sulfurreducens* biofilms grown in the QCM cell. To better understand the frequency shift/potential response, we removed a portion of the visible biofilm, as shown in Figure SI-1 in the Supporting Information. Figure 7B shows the resulting response as the limiting current was reduced from 130 to $55 \mu\text{A}$ as about 50% of the visible biofilm was removed and slightly above zero current when 100% of the visible biofilm was removed. At the same time, the frequency shift was reduced from -92 to -32 Hz and finally to -4 Hz when about 50 and 100% of the visible biofilm was removed, respectively. Therefore, from the results shown in Figure 7A and B, it is clear that the decrease in frequency shift towards oxidizing potentials (limiting current) is related to the state of the biofilm. Increasing biofilm attachment increased the frequency shift, and removal of biofilm decreased the frequency shift. The decrease in frequency shift upon current flow suggests that the biofilm is increasing in apparent mass. Therefore, we suspected that either the biofilm mass was changing or the structure (viscoelastic properties) was changing during cyclic voltammograms similar to PANI films.^[24] By considering the timescale of CV ($\approx 6 \text{ min}$), it is unlikely that more biofilm attachment causes the change. When the visible biofilm was removed, the overall frequency shift changed correspondingly with the amount of visible biofilm removed.

To assess whether electron flux was the cause of the frequency shift during CV, we measured the frequency shift/potential response under both turnover and nonturnover conditions in which acetate (electron donor) was removed. Figure 8A shows a limiting current of $120 \mu\text{A}$ and a frequency shift of -440 Hz at oxidizing potentials under turnover conditions. When the biofilm was brought to nonturnover conditions, the usual *G. sulfurreducens* biofilm CV was observed, with multiple anodic and cathodic peaks.^[2a] Although catalytic current had decreased to background levels, a frequency shift of -85 Hz was still observed at oxidizing potentials. This

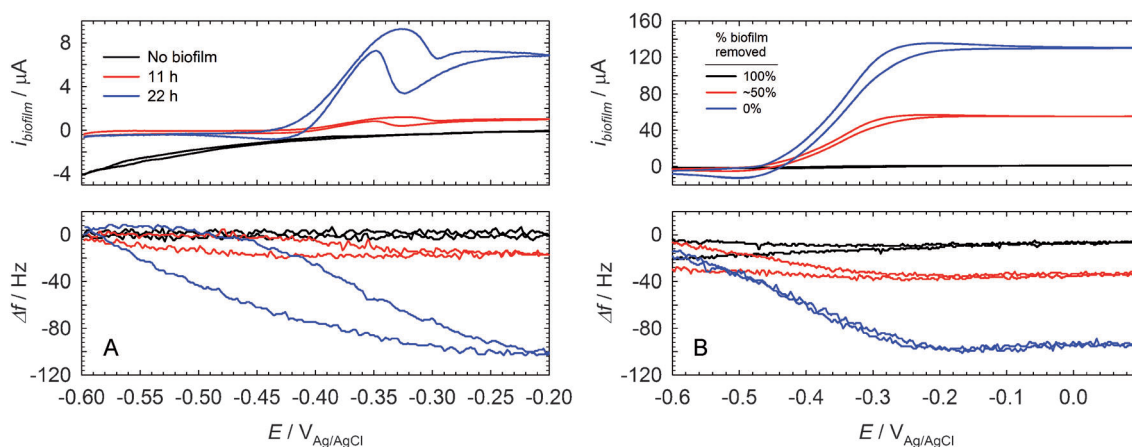


Figure 7. Cyclic voltammograms (top) and corresponding frequency shift response (bottom) of *G. sulfurreducens* biofilm A) during initial growth and B) after visible biofilm was removed.

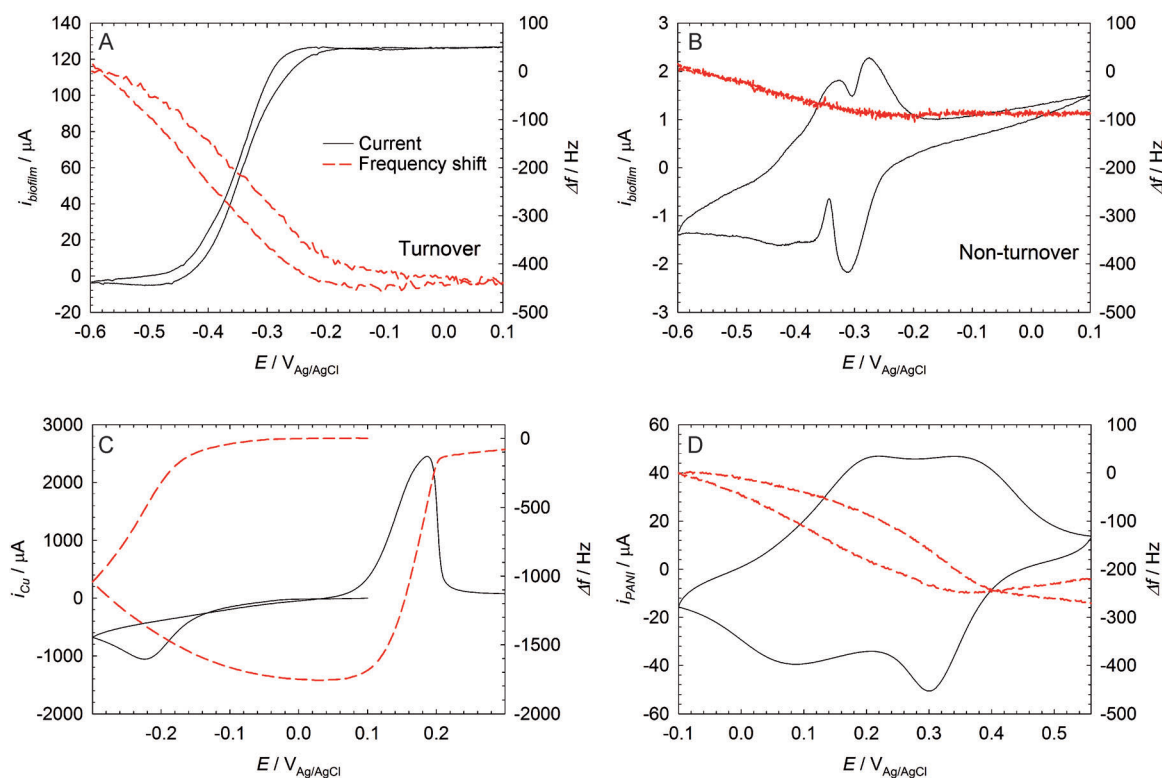


Figure 8. Cyclic voltammograms and corresponding frequency shift responses of *G. sulfurreducens* biofilm under A) turnover and B) nonturnover conditions. C) Copper deposition in a solution of copper sulfate during CV. D) Cyclic voltammogram of electrodeposited PANI film.

means that, although the frequency shift/potential response was predominately caused by electron flux through the biofilm (Δ of 355 Hz), there was still a residual amount of frequency shift caused by the change from a reduced to an oxidized state of the biofilm. Furthermore, scanning as slow as 0.1 mVs^{-1} , as shown in Figure SI-2 in the Supporting Information, did not remove the frequency shift response.

2.5. The Cause of this Frequency Shift Behavior in *G. sulfurreducens* Biofilms

In an effort to elucidate the observed frequency response, we considered three different electrochemical reaction systems: 1) metal deposition during CV, 2) PANI oxidation/reduction during CV, and 3) ferri-/ferrocyanide oxidation/reduction during CV. The choice of reaction systems was fairly clear, because the first results in a thin, rigid metal film, the second results in a thick, conductive polymer film, and the third is an example of a diffusing, non-film-forming reaction. In Figure 8C, the frequency shift is dominated by the plating of copper on the gold surface as copper ions are reduced to solid copper. The frequency remains depressed until the copper is stripped off on the return scan. Notably, the frequency shift for the metal is approximately -1700 Hz , which is much larger than the biofilm response. In Figure 8D, the frequency is depressed at more positive potentials when the PANI film is oxidized. As PANI is p doped, solvent incorporation is primarily related to the doping of the film, such that, when the PANI film is reduced, solvent is expelled.^[24] As no PANI can be electrodeposit-

ed at these potentials (i.e. less than the steady potential in Figure 4), the frequency shift is purely a consequence of changes in the film properties with potential and not of the deposition of mass. Thus, if we compare the biofilm to these two opposite cases, we find that qualitatively the biofilm is closer to the PANI film in frequency shift response during CV. This tells us that *G. sulfurreducens* biofilms, similar to PANI films, require a quantifiable amount of ingress/egress of solvent during electron transfer or undergo significant structural changes in the biofilm. Therefore, the similarity between the two films during CV supports the need for researchers to consider a change in film properties during electron transfer, complicating electron-transfer mechanisms inside *G. sulfurreducens* biofilms above what is already considered a multistep process. Finally, less exciting and expected was the frequency shift/potential response of the ferricyanide case shown in Figure SI-3 in the Supporting Information. Approximately -20 Hz was observed at oxidizing potentials, which might have simply reflected the change in the double layer as the potential was swept.

2.6. Relating Frequency Shift to Diffusion Coefficients in *G. sulfurreducens* Biofilms

We previously measured diffusion coefficients inside electrorespiring *G. sulfurreducens* biofilms by using electrochemical NMR spectroscopy and showed that the dense nature of *G. sulfurreducens* biofilms caused effective diffusion coefficients (D_e) to drop significantly.^[12b] Of particular interest to this study is the observation that D_e can be altered by simply halting the

polarization and subsequently biofilm respiration. Under current flow, D_e increased; under no current flow, D_e decreased. This change was not caused by electromigration (see Ref. [12b]) and was thought to be caused by a change in morphology and the biofilm microstructure, which was left undetermined. As the incorporation of solvent would cause biofilm density to decrease, the frequency shift response we observed herein under turnover conditions was likely to be the same response, in which D_e increased with current. This means that the mass flux inside the biofilm increases substantially, such that these changes can be observed by using a QCM. Therefore, QCM is a critical tool for assessing biofilm properties that are not observed by using electrochemical means. Furthermore, under no current flow or nonturnover conditions, the biofilm frequency shift was nonzero, which indicated that an alteration of the film properties occurred. Such a finding could allude to the protonation/deprotonation of key structures inside *G. sulfurreducens* biofilms, such as c-type cytochromes.^[2b,25]

2.7. Frequency Shift and Apparent Mass of the Biofilm

The QCM provided an unprecedented amount of information about the native state of electrode-respiring *G. sulfurreducens* biofilms in relation to their initial attachment, growth, and oxidation state. Generally, the Sauerbrey relationship^[10] [Eq. (1)] is used to convert the changes in resonant frequency of an oscillating QCM electrode into mass:

$$\Delta f = -\frac{2f_o^2}{A\sqrt{\rho_q\mu_q}}\Delta m \quad (1)$$

in which Δf is the frequency shift (in Hz), f_o is the principal series resonant frequency (in Hz), A is the area between electrodes (in cm^2), ρ_q is the AT-cut quartz crystal density (in g cm^{-3}), μ_q is the shear modulus of the AT-cut quartz crystal, and Δm is the mass change (in g). For mass (for which the small load approximation applies) on a QCM that can be considered theoretically as an extension of the quartz crystal, Equation (1) applies. For viscoelastic films, a viscosity correction factor is used to modify Equation (1).^[26] In the absence of bandwidth measurements, it is difficult to employ such correction factors. By considering Equation (1), however, we can qualitatively observe the change in biofilm elasticity over time. Figure 9A–C shows the series frequency shift and parallel frequency shift for copper deposition, PANI electrodeposition, and biofilm growth. For all three cases, both initial series and parallel frequency shifts follow each other closely. As mass is deposited, the parallel frequency shift tends away from the series resonant frequency shift. At a series resonant frequency shift of -1000 Hz, the parallel frequency shifts for copper, PANI, and the biofilm are -891 , -721 , and 741 Hz, respectively. The differences between the series resonant frequency shift and parallel resonant frequency shift are then 108, 279, and 1741 Hz for copper, PANI, and the biofilm, respectively. Essentially, biofilms are not comparable with copper and PANI films, because

of the viscoelastic nature of the films.^[11] The application of Equation (1) to *G. sulfurreducens* biofilms should, thus, be avoided.

Although we have discussed the implications of the viscoelastic nature of *G. sulfurreducens* biofilms on QCM electrodes and the inability to measure a quantitative mass value, the fact that the series resonant frequency shift is linear with respect to current implies that the QCM response can be used to assess the film properties in addition to the electrochemical properties of a biofilm. In particular, we can use the QCM to interrogate the coupled processes of ion flux during electron transfer.^[15] The visible change in frequency shift during CV of *G. sulfurreducens* biofilms points to the importance of the flux not

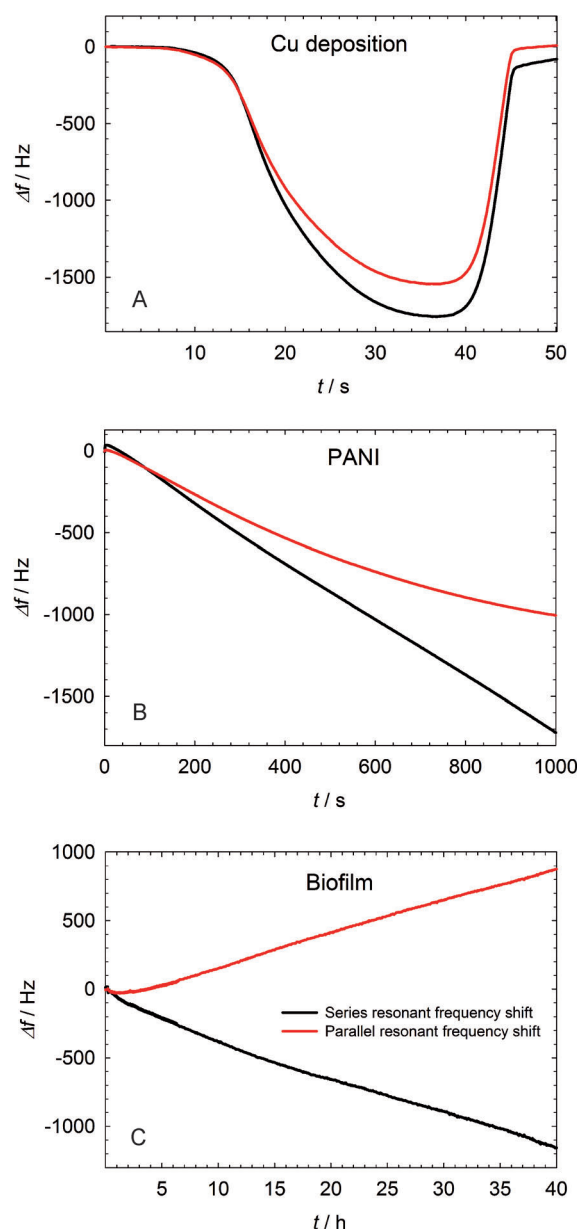


Figure 9. Series and parallel frequency shifts for A) copper deposition, B) PANI electrodeposition, and C) biofilm growth. Rigid films on the QCM surface exhibit small differences between series and parallel frequency shifts, whereas nonrigid films exhibit large differences.

only of charge species,^[4a,27] but also of neutral species/solvent as well.^[15] We present the first direct evidence, by using the QCM, that the movement of solvent in *G. sulfurreducens* biofilms plays an important role in the overall electron-transfer rates. This is corroborated by previous measurements of diffusion coefficients and biofilm imaging by using nuclear magnetic resonance (NMR) spectroscopy methods.^[12b] Furthermore, one potential application of the QCM for monitoring *G. sulfurreducens* and other electrochemically active biofilms is shown in Figure 10. The frequency shift response with current can be

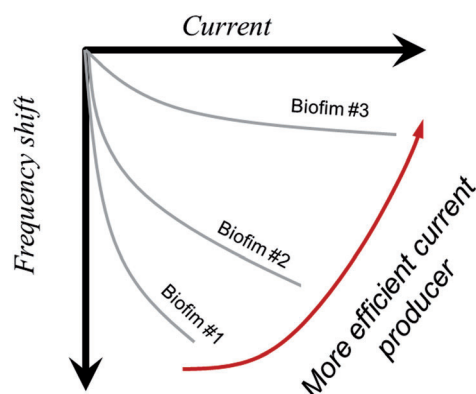


Figure 10. Possible application of QCM to determine the most efficient current producer for electrochemically active biofilms. Frequency shift could be used to normalize current responses between different biofilm types.

assessed for multiple biofilm replicates, mutations of biofilm, cross-species analysis, or multispecies analysis to determine whether any changes in the film properties are the cause of electron-transfer rate differences. This could also explain macroscopic changes in microbial fuel cell performance, in which shear stress improves the performance of the anode.^[28] These changes could be observed by the QCM. If we define the most efficient current producer to be the electrochemically active biofilm that has the smallest frequency shift, then engineering attempts could benefit from QCM studies. However, we realize that significant effort is required to realize this application of QCM to electrochemically active biofilms.

3. Conclusions

We grew *G. sulfurreducens* biofilms on QCM electrodes and found that, in the short term, frequency shift was linear with respect to current for the biofilm, which was different from PANI, for which frequency shift was linear with respect to charge. In long-term biofilm growth up to the exponential phase, there was a second linear region of frequency shift with respect to current. During CV, there was a reproducible, negative increase in frequency shift at oxidizing potentials. The frequency shift was dependent on the steady-state current (biofilm growth) and availability of an electron donor. However, it did not disappear under nonturnover conditions, which indicated that the oxidation state of the biofilm caused a change in the film properties of the biofilm. The frequency response

during CV of the biofilm was most like the response of PANI. As measured in both series and parallel frequency shifts, the biofilm was qualitatively more viscoelastic than both copper and PANI films. This meant that the Sauerbrey relationship was not applicable for the biofilm and frequency shift should not be represented as mass changes to avoid misleading statements. QCM may be used in applications in which it is useful to find the most efficient current producer.

Experimental Section

Abbreviated QCM Theory

QCM takes advantage of AT-cut quartz crystals operated near their fundamental frequency of vibration, which can be visualized by examining the equivalent electrical circuit in Figure 11. We used equivalent electrical circuits herein to facilitate a broader under-

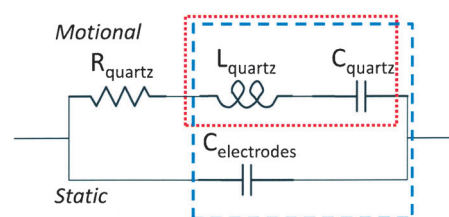


Figure 11. Equivalent electrical circuit representation of the QCM crystal operating at the fundamental frequency. The red dotted box represents the source of the series frequency shift, and the blue dashed box represents the source of the parallel frequency shift. Motional refers to the *RLC* behavior caused by the quartz resonance (*R*: resistance, *L*: inductance, *C*: capacitance). Static refers to the capacitance caused by the overlap between gold electrodes, which is not caused by the quartz resonance.

standing of resonant frequencies without cumbersome derivations. The derivation and theoretical treatment can be found elsewhere in several forms.^[9,26] The origin of the resonance in QCM lies in the series LC portion (red dotted box) of the motional branch in Figure 11. In this electromechanical perspective, the inductance refers to inertia and the capacitance refers to elasticity of the oscillating crystal. The resistive element, representing viscous losses, adds a damping factor characteristic of series *RLC* electrical circuits. $C_{\text{electrodes}}$ refers to the electrical capacitance formed between the gold electrodes and the quartz crystal and is considered the static branch. The inclusion of the parallel capacitance, $C_{\text{electrodes}}$ (blue dashed box), gives rise to a second resonant frequency. Thus, two resonant frequencies, conveniently described as the series and parallel resonant frequencies, can be monitored. The series and parallel resonant frequencies are related to a good degree of approximation^[9] by Equation (2):

$$\frac{f_p - f_s}{f_s} = \frac{C_{\text{quartz}}}{2C_{\text{electrodes}}} \quad (2)$$

in which f_p is the parallel resonant frequency and f_s is the series resonant frequency. From Equation (2), the separation of f_p and f_s can provide qualitative clues about elastic changes to the oscillating crystal. We also note that a third parameter, the bandwidth of the equivalent electrical circuit, can also be monitored by using the method of QCM with dissipation (QCM-D).^[7,26]

Frequency shift in QCM refers to changes in the resonant frequency of the oscillating crystal due to loading or attachment of a film, such that the frequency shift is much smaller than the fundamental frequency of the crystal. Therefore, the impedance of the attached film is much smaller than the impedance of the equivalent electrical circuit in Figure 11 and this defines the small load approximation.^[9] When the small load approximation is valid, the frequency shift will represent changes in the loading of the oscillating crystal. Because biofilms exhibit viscoelastic behavior, the frequency shift is likely to comprise changes in the mass, viscosity, and elasticity of the biofilm. Herein, the qualitative changes in biofilm properties were tracked with time through the frequency shifts of both the series and parallel resonant frequencies. Although quantitative determinations were not made herein, qualitative understanding of biofilm changes was acquired by using comparisons with known systems, which include copper deposition, PANI electrodeposition, and non-film-forming ferricyanide reduction.

Bioelectrochemical Cell

Biofilms were grown in a continuously fed, temperature-controlled electrochemical cell, exactly as previously published,^[29] except the working electrode was the QCM electrode. Briefly, the working electrode, on which *G. sulfurreducens* respired, was a gold disk (0.385 cm²) that also functioned as one face of a 10 MHz Au crystal (Gamry Instruments #971-00019). Only one face of the gold-coated crystal was exposed to solution, whereas the rest of the surface was insulated by a plastic coating. The QCM crystal was used as is and was mounted in the cell by using a crystal holder (eSorption Probe, Gamry Instruments #971-00018). The counter electrode was a graphite rod (Sigma-Aldrich #496545), and the reference electrode was a saturated Ag/AgCl reference. The electrochemical cell (Gamry Instruments #990-00249) was modified to allow continuous feeding. Norprene tubing (Cole-Parmer #EW-06404-14 and #EW-06404-13) was used for the feed and waste streams, respectively. Flow breakers were used in the feed and waste streams to prevent back contamination. A 0.2 μm filter was used at the gas inlet to sparge a mixture of N₂/CO₂ (80%/20%). The gas inlet pressure was adjusted slightly above the water column pressure in the cell to provide positive pressure without vigorous mixing by rising gas bubbles. Another 0.2 μm filter was used at the gas outlet to relieve pressure buildup. The entire setup, except for the reference and working electrodes, was autoclaved for 20 min at 121 °C. The growth medium was autoclaved separately in a 1 L autoclavable glass bottle for 100 min at 121 °C. Once the cell and growth media cooled to room temperature, the growth medium bottle was aseptically connected to the cell feed stream. Working and reference electrodes were placed in 70% v/v ethanol in deionized water for 45 min under UV exposure before being placed inside the cell. A temperature controller was used to maintain a cell temperature of 30 °C by using the glass jacket. A mixture of N₂/CO₂ (80%/20%) gas was then sparged for 24 h.

Growth Medium

The growth medium used to grow *G. sulfurreducens* strain PCA (ATCC 51573) biofilms consisted of potassium chloride (0.38 g L⁻¹), ammonium chloride (0.2 g L⁻¹), sodium phosphate monobasic (0.069 g L⁻¹), calcium chloride (0.04 g L⁻¹), magnesium sulfate heptahydrate (0.2 g L⁻¹), sodium carbonate (2 g L⁻¹), Wolfe's vitamin solution (10 mL L⁻¹), and modified Wolfe's mineral solution (10 mL L⁻¹). Acetate (20 mM) was provided as the electron donor. No fumarate or other soluble electron acceptor was added to the growth medium used to grow biofilms.

eQCM Operation

An eQCM 10M QCM (Gamry Instruments, #992-00083) was interfaced with a Gamry Series G300 potentiostat (Gamry Instruments, Warminster, PA, USA) to simultaneously monitor series resonance frequency, parallel resonance frequency, and current in real time. Initially, the sterilized quartz crystal was placed inside the cell, followed by the introduction of sterile growth medium. Background series and parallel resonant frequencies were obtained while the working electrode was polarized to 0 V_{Ag/AgCl}. The polarization potential was chosen to provide the limiting current (see Figure 1, inset), at which 0 V_{Ag/AgCl} was a few hundred millivolts beyond the onset of limiting current. CV was run by using the same equipment without any physical modification to the system.

Biofilm Growth

Once a steady background was observed for series resonance frequency, parallel resonant frequency, and current, *G. sulfurreducens* inoculum was added to the cell by following a previously published method.^[29] The cell volume was 115 mL. The dilution rate of the cell was 0.01 h⁻¹ (or a flow rate of ≈1 mL h⁻¹). Non-turnover conditions were achieved after the medium was replaced with acetate-free medium and the biofilm was starved for an additional 48 h. During nonturnover conditions, no catalytic current was generated. This was verified by CV. Overall, three independent biological replicates were run, which gave the same conclusions presented. For clarity, we show only representative data.

PANI, Copper Deposition, and Ferricyanide Experiments

Because these experiments were abiotic, they were conducted in a static eQCM Teflon cell (Gamry, #971-00003) with similar gold-coated quartz crystals (Gamry, #971-00006). The same eQCM setup was used as that in the bioelectrochemical cell setup. For electrodeposition of PANI, aniline HCl (Sigma-Aldrich #10414-50G-F) was dissolved in 18 MΩ cm⁻¹ water to a concentration of 0.1 M. The solution of aniline HCl was added to the eQCM Teflon cell with a Pt counter electrode and a saturated Ag/AgCl reference electrode. Background series and parallel resonant frequency shifts were obtained before galvanostatic deposition of PANI at a current of 1 μA for the results shown in Figure 4 and 10 μA for the results shown in Figure 5B. Series resonant frequency, parallel resonant frequency, and potential were recorded during electrodeposition. Once electrodeposition had ended, the solution of aniline HCl was replaced with 0.1 M HCl and cyclic voltammograms of the PANI film were obtained as series and parallel resonant frequencies were recorded. Solutions of 10 mM copper sulfate in 1 M H₂SO₄ were used to form copper films on the quartz crystal. Initially, no copper was plated onto the QCM crystal. When the potential was swept at 50 mV s⁻¹ in the negative direction by using CV, Cu^{II} was deposited onto the surface. On the sweep back, Cu was released back into solution. Ferricyanide was used as a control for a non-film-forming electrochemical reaction. Potassium ferricyanide(III) (Sigma-Aldrich #244023-500G) was dissolved in 0.1 M HCl to a final concentration of 0.1 M. CV was run similar to the conditions in the PANI case.

SEM Sample Preparation

The QCM disk was removed from the cell with biofilm sample attached and immediately placed into a fixation solution containing 2.5% glutaraldehyde and 2% paraformaldehyde in 0.1 M sodium phosphate buffer. Fixation was performed overnight at 4 °C. Prior to dehydration, the fixation solution was gently removed and re-

placed with 0.1 M sodium phosphate buffer. After 10 min incubation, the buffer was replaced. This was repeated to give three buffer rinses. This was followed by dehydration with 10 min at each of the following concentrations of ethanol: 30, 50, 70, and 95%. Finally, 3 × 10 min incubations at 100% ethanol were performed. The sample was dried by removing the last ethanol rinse and replacing it with hexamethyldisilazane (HMDS). This was left overnight at room temperature. After the sample was critically dried, a sputter coater was used to coat this sample with 150–200 Å of gold.

Acknowledgements

This research is supported by the U.S. Office of Naval Research (ONR), grant no. N00014-09-1-0090. J.T.B. was also supported through an internship with Gamry Instruments, Inc. We acknowledge Emily K. Davenport for SEM imaging of the biofilms and the Franceschi Microscopy and Imaging Center of Washington State University for the use of their facilities and staff assistance.

Keywords: bacteria · biofilms · cyclic voltammetry · electrochemistry · quartz crystal microbalance

- [1] a) J. K. Fredrickson, J. M. Zachara, *Geobiology* **2008**, *6*, 245–253; b) D. R. Lovley, *Geobiology* **2008**, *6*, 225–231.
- [2] a) K. Fricke, F. Harnisch, U. Schroder, *Energy Environ. Sci.* **2008**, *1*, 144–147; b) R. M. Snider, S. M. Strycharz-Glaven, S. D. Tsoi, J. S. Erickson, L. M. Tender, *Proc. Natl. Acad. Sci. USA* **2012**, *109*, 15467–15472; c) E. Marsili, J. Sun, D. R. Bond, *Electroanalysis* **2010**, *22*, 865–874; d) G. Reguera, K. P. Nevin, J. S. Nicoll, S. F. Covalla, T. L. Woodard, D. R. Lovley, *Appl. Environ. Microbiol.* **2006**, *72*, 7345–7348.
- [3] J. Babauta, R. Renslow, Z. Lewandowski, H. Beyenal, *Biofouling* **2012**, *28*, 789–812.
- [4] a) A. E. Franks, K. P. Nevin, H. F. Jia, M. Izallalen, T. L. Woodard, D. R. Lovley, *Energy Environ. Sci.* **2009**, *2*, 113–119; b) N. Lebedev, S. M. Strycharz-Glaven, L. M. Tender, *ChemPhysChem* **2014**, *15*, 320–327.
- [5] a) J. Gutman, S. L. Walker, V. Freger, M. Herzberg, *Environ. Sci. Technol.* **2013**, *47*, 398–404; b) A. Bressel, J. W. Schultze, W. Khan, G. M. Wolf-aardt, H. P. Rohns, R. Irmscher, M. J. Schöning, *Electrochim. Acta* **2003**, *48*, 3363–3372; c) I. Gall, M. Herzberg, Y. Oren, *Soft Matter* **2013**, *9*, 2443–2452.
- [6] a) D. Q. Jiang, B. K. Li, W. Z. Jia, Y. Lei, *Appl. Biochem. Biotechnol.* **2010**, *160*, 182–196; b) J. M. Kleijn, Q. Lhuillier, A. W. Jeremiasse, *Bioelectrochemistry* **2010**, *79*, 272–275.
- [7] S. T. Brown-Malker, S. Read, A. Rowlands, J. Cooper-White, J. Keller, *ECS Trans.* **2010**, *28*, 11–22.
- [8] D. G. G. McMillan, S. J. Marritt, M. A. Firer-Sherwood, L. Shi, D. J. Richardson, S. D. Evans, S. J. Elliott, J. N. Butt, L. J. C. Jeuken, *J. Am. Chem. Soc.* **2013**, *135*, 10550–10556.
- [9] D. Salt, *Hy-Q Handbook of Quartz Crystal Devices*, Van Nostrand Reinhold, Wokingham, **1987**.
- [10] G. Sauerbrey, *Z. Phys.* **1959**, *155*, 206–222.
- [11] P. Stoodley, Z. Lewandowski, J. D. Boyle, H. M. Lappin-Scott, *Biotechnol. Bioeng.* **1999**, *65*, 83–92.
- [12] a) Y. Liu, H. Kim, R. R. Franklin, D. R. Bond, *ChemPhysChem* **2011**, *12*, 2235–2241; b) R. S. Renslow, J. T. Babauta, P. D. Majors, H. Beyenal, *Energy Environ. Sci.* **2013**, *6*, 595–607.
- [13] N. S. Malvankar, M. Vargas, K. P. Nevin, A. E. Franks, C. Leang, B. C. Kim, K. Inoue, T. Mester, S. F. Covalla, J. P. Johnson, V. M. Rotello, M. T. Tuominen, D. R. Lovley, *Nat. Nanotechnol.* **2011**, *6*, 573–579.
- [14] K. Lee, S. Cho, S. H. Park, A. J. Heeger, C.-W. Lee, S.-H. Lee, *Nature* **2006**, *441*, 65–68.
- [15] A. R. Hillman, M. J. Swann, S. Bruckenstein, *J. Phys. Chem.* **1991**, *95*, 3271–3277.
- [16] D. R. Bond, D. R. Lovley, *Appl. Environ. Microbiol.* **2003**, *69*, 1548–1555.
- [17] G. Reguera, K. D. McCarthy, T. Mehta, J. S. Nicoll, M. T. Tuominen, D. R. Lovley, *Nature* **2005**, *435*, 1098–1101.
- [18] I. Sapurina, J. Stejskal, *Polym. Int.* **2008**, *57*, 1295–1325.
- [19] E. Sabatani, Y. Gafni, I. Rubinstein, *J. Phys. Chem.* **1995**, *99*, 12305–12311.
- [20] X. Jiang, J. Hu, E. R. Petersen, L. A. Fitzgerald, C. S. Jackan, A. M. Lieber, B. R. Ringeisen, C. M. Lieber, J. C. Biffinger, *Nat. Commun.* **2013**, *4*, 2751.
- [21] J. S. McLean, G. Wanger, Y. A. Gorby, M. Wainstein, J. McQuaid, S. I. Ishii, O. Bretschger, H. Beyenal, K. H. Nealson, *Environ. Sci. Technol.* **2010**, *44*, 2721–2727.
- [22] K. P. Nevin, B. C. Kim, R. H. Glaven, J. P. Johnson, T. L. Woodard, B. A. Methe, R. J. DiDonato, S. F. Covalla, A. E. Franks, A. Liu, D. R. Lovley, *PLoS One* **2009**, *4*, e5628.
- [23] N. S. Malvankar, M. T. Tuominen, D. R. Lovley, *Energy Environ. Sci.* **2012**, *5*, 5790–5797.
- [24] E. Sabatani, A. Redondo, J. Rishpon, A. Rudge, I. Rubinstein, S. Gottesfeld, *J. Chem. Soc. Faraday Trans.* **1993**, *89*, 287–294.
- [25] L. Morgado, V. B. Paixao, M. Schiffer, P. R. Pokkuluri, M. Bruix, C. A. Salgueiro, *Biochem. J.* **2012**, *441*, 179–187.
- [26] D. Johannsmann, *Phys. Chem. Chem. Phys.* **2008**, *10*, 4516–4534.
- [27] C. I. Torres, A. K. Marcus, B. E. Rittmann, *Biotechnol. Bioeng.* **2008**, *100*, 872–881.
- [28] H. T. Pham, N. Boon, P. Aelterman, P. Clauwaert, L. De Schampelaire, P. Van Oostveldt, K. Verbeken, K. Rabaey, W. Verstraete, *Microb. Biotechnol.* **2008**, *1*, 487–496.
- [29] J. T. Babauta, H. Beyenal, *Biotechnol. Bioeng.* **2014**, *111*, 285–294.

Received: May 11, 2014

Revised: June 17, 2014

Published online on August 8, 2014